

## Evidence for Valencelike Quark-Hadron Duality

I. Niculescu,<sup>1</sup> C. S. Armstrong,<sup>2</sup> J. Arrington,<sup>3</sup> K. A. Assamagan,<sup>1</sup> O. K. Baker,<sup>1,5</sup> D. H. Beck,<sup>4</sup> C. W. Bochna,<sup>4</sup>  
 R. D. Carlini,<sup>5</sup> J. Cha,<sup>1</sup> C. Cothran,<sup>6</sup> D. B. Day,<sup>6</sup> J. A. Dunne,<sup>5</sup> D. Dutta,<sup>7</sup> R. Ent,<sup>5</sup> V. V. Frolov,<sup>8</sup> H. Gao,<sup>4</sup>  
 D. F. Geesaman,<sup>9</sup> P. L. J. Gueye,<sup>1</sup> W. Hinton,<sup>1</sup> R. J. Holt,<sup>4</sup> H. E. Jackson,<sup>9</sup> C. E. Keppel,<sup>1,5</sup> D. M. Koltenuk,<sup>12</sup> D. J. Mack,<sup>5</sup>  
 D. G. Meekins,<sup>2,5</sup> M. A. Miller,<sup>4</sup> J. H. Mitchell,<sup>5</sup> R. M. Mohring,<sup>10</sup> G. Niculescu,<sup>1</sup> D. Potterveld,<sup>9</sup> J. W. Price,<sup>8</sup>  
 J. Reinhold,<sup>9</sup> R. E. Segel,<sup>7</sup> P. Stoler,<sup>8</sup> L. Tang,<sup>1,5</sup> B. P. Terburg,<sup>4</sup> D. Van Westrum,<sup>11</sup> W. F. Vulcan,<sup>5</sup> S. A. Wood,<sup>5</sup>  
 C. Yan,<sup>5</sup> and B. Zeidman<sup>9</sup>

<sup>1</sup>*Hampton University, Hampton, Virginia 23668*

<sup>2</sup>*College of William and Mary, Williamsburg, Virginia 23187*

<sup>3</sup>*California Institute of Technology, Pasadena, California 91125*

<sup>4</sup>*University of Illinois at Urbana-Champaign, Urbana, Illinois 61801*

<sup>5</sup>*Thomas Jefferson National Accelerator Facility, Newport News, Virginia 23606*

<sup>6</sup>*University of Virginia, Charlottesville, Virginia 22901*

<sup>7</sup>*Northwestern University, Evanston, Illinois 60201*

<sup>8</sup>*Rensselaer Polytechnic Institute, Troy, New York 12180*

<sup>9</sup>*Argonne National Laboratory, Argonne, Illinois 60439*

<sup>10</sup>*University of Maryland, College Park, Maryland 20742*

<sup>11</sup>*University of Colorado at Boulder, Boulder, Colorado 80309*

<sup>12</sup>*University of Pennsylvania, Philadelphia, Pennsylvania 19104*

(Received 14 May 1999; revised manuscript received 4 April 2000)

A newly obtained data sample of inclusive electron-nucleon scattering from both hydrogen and deuterium targets is analyzed. These JLab data span the nucleon resonance region up to four-momentum transfers of 5 (GeV/c)<sup>2</sup>. The data are found to follow an average scaling curve. The inclusion of low-momentum transfer data yields a scaling curve resembling deep inelastic neutrino-nucleus scattering data, suggesting a sensitivity to valencelike structure only.

PACS numbers: 13.60.Hb, 12.38.Qk

Nearly 30 years ago Bloom and Gilman observed that the electroproduction of resonances resembles the scaling behavior of the deep inelastic structure function, if expressed in terms of a scaling variable connecting the two different kinematic regions, and if averaged over a large range of invariant mass  $W$  [1]. It was suggested that this relationship between resonance electroproduction and the deep inelastic scattering hinted at a common origin for both phenomena, called local duality. A quantitative quantum chromodynamics (QCD) analysis of this empirical observation was given by De Rujula, Georgi, and Politzer [2]. They showed that the resonances oscillate around an *average* scaling curve. Although electroproduction of resonances is a strongly non-perturbative phenomenon, the resonance strengths average to a global scaling curve, resembling the deep inelastic scaling curve, as the higher-twist effects are not large, if averaged over a large kinematic region.

Higher-twist effects can be viewed as processes where the struck quark communicates with one or more of the spectator quarks by gluon exchange. In the deep inelastic  $F_2$  data, higher-twist terms have been found to be small for Bjorken  $x < 0.40$  [3], and insignificant for  $x \approx 0.01$ , even at  $Q^2 \approx 1$  (GeV/c)<sup>2</sup>, where  $Q$  is the four-momentum transfer [4,5]. On the other hand, gauge invariance requires  $F_2$  to vanish linearly with  $Q^2$  at  $Q^2 = 0$  (GeV/c)<sup>2</sup> [6], suggesting nonperturbative effects govern this region.

In this Letter we assume higher-twist effects, if averaged over the full resonance region, to be small, even at relatively low-momentum transfers, and thus local duality to remain valid. A quantitative verification of this assumption will be presented elsewhere [7].

A sample of high-precision data in the nucleon resonance region, in combination with substantial progress made over the last 20 years in determining the scaling behavior of deep inelastic structure functions with electron, muon, and neutrino probes, enables us to revisit local duality in detail. We investigate the connection between resonance electroproduction and deep inelastic scattering to lower four-momentum transfers than previously investigated, and consider possible implications.

We accumulated data in the nucleon resonance region,  $1 < W^2 < 4$  GeV<sup>2</sup>, for both hydrogen and deuterium targets [8]. Measurements in the elastic region were included in the data to verify our absolute normalizations to better than 2%. The data were obtained in Hall C at Jefferson Lab (JLab), using electron beam energies between 2.4 and 4 GeV. Incident beam currents between 20 and 100  $\mu$ A were used on 4 and 15 cm long targets. Scattered electrons were detected in both the high momentum spectrometer and the short orbit spectrometer [8], each utilized in a single arm mode to measure the inclusive cross sections. At all beam energy-scattering angle combinations, the central momentum of the spectrometers was varied to

cover the full resonance region. The  $Q^2$  range covered by our data set is between 0.3 and 5 (GeV/c)<sup>2</sup>. The overall systematic uncertainty in the measured cross sections due to target density, beam charge, beam energy, spectrometer acceptance, radiative corrections, and detection efficiency is 3.5% and larger than the statistical uncertainties [8–10].

We extracted the structure function  $F_2$  from the measured differential cross sections  $\sigma = \frac{d^3\sigma}{d\Omega dE'}$  like  $F_2 \sim \sigma \times (1 + R)/(1 + \epsilon R)$  [11]. Here  $\epsilon$  is the virtual-photon polarization and  $R$  the ratio of longitudinal to transverse cross sections. We used a value of  $R = 0.2$ , but the results are consistent within 2% if a parametrization of this quantity based on deep inelastic scattering data at moderate  $Q^2$  is utilized [12]. However, we note that this quantity is presently known only at the  $\pm 100\%$  level in the nucleon resonance region above  $Q^2 \approx 1$  (GeV/c)<sup>2</sup>.

Samples of the extracted  $F_2$  data in the nucleon resonance region are shown in Fig. 1a for the hydrogen target and in Fig. 1b for the deuterium target, as functions of the Nachtmann scaling variable  $\xi$ . These figures also include some low  $Q^2$  data from SLAC [13,14]. In terms of the Nachtmann variable  $\xi = 2x/(1 + \sqrt{1 + 4M^2x^2/Q^2})$  [15], where  $M$  is the nucleon mass, a pattern of scaling violations has been formulated within a QCD framework [2]. The variable  $\xi$  takes target-mass corrections into account, necessary as the quarks cannot be treated as massless partons for low to moderate momentum transfers. Note that, for low  $x$  or large  $Q^2$ , the scaling variable  $\xi$  is almost identical to the Bjorken scaling variable  $x$ .

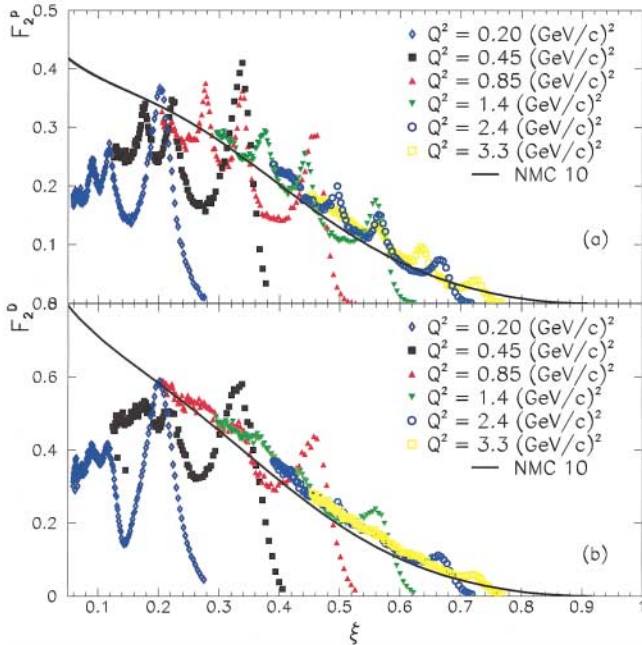


FIG. 1 (color). Extracted  $F_2$  data in the nucleon resonance region for hydrogen (a) and deuterium (b) targets, as functions of the Nachtmann scaling variable  $\xi$ . For clarity, only a selection of the data is shown here. The solid curves indicate the result of the NMC fit to deep inelastic data for a fixed  $Q^2 = 10$  (GeV/c)<sup>2</sup> [16].

It is clear from Fig. 1 that the data oscillate around a global curve. This reiterates the well-known local duality picture; the data at various values of  $Q^2$  and  $W^2$  average to a smooth curve if expressed in terms of  $\xi$ . The solid curve shown is a global fit to the world's deep inelastic data by the New Muon Collaboration (NMC) [16] for a fixed  $Q^2 = 10$  (GeV/c)<sup>2</sup> (NMC10, solid). Previous analyses of local duality have concentrated on a comparison of deep inelastic constrained curves with nucleon resonance data for  $Q^2 \geq 1$  (GeV/c)<sup>2</sup>, corresponding to a lower cutoff of  $\xi \approx 0.3$ . However, as one can see from Fig. 1, the resonance data still seem to oscillate around a global curve, even in the region  $\xi \leq 0.3$ . This suggests that also in this region the effect of the higher-twist terms is reduced if *averaged* over the full resonance region—consistent with the earlier QCD analysis of the  $\xi > 0.3$  region [2]. Note that, for sake of visual clarity, we did not include all spectra.

From now on we will concentrate on the region of  $\xi \leq 0.3$ . We initially construct a scaling curve representing the *average* of the resonance data in the region  $M^2 \leq W^2 < 4$  GeV<sup>2</sup>, for  $Q^2 < 5$  (GeV/c)<sup>2</sup>. The average curve for the hydrogen data is shown as a shaded band in Fig. 2, where the width of the band takes the systematic uncertainties of the procedure into account. Note that the

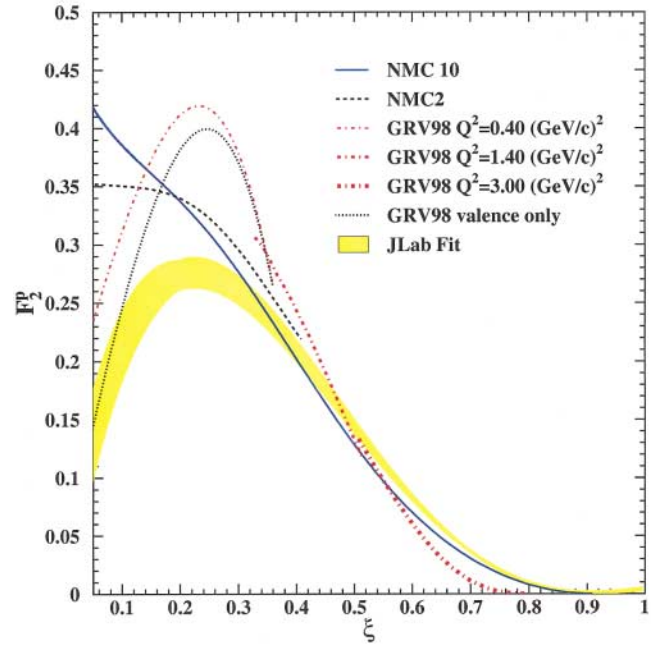


FIG. 2 (color). The shaded band indicates the  $F_2$  scaling curve obtained by averaging over all the proton resonance data (see text). The width indicates the uncertainty in the averaging procedure. The solid (dashed) curve indicates the result of the NMC fit to deep inelastic data for a fixed  $Q^2 = 10$  (GeV/c)<sup>2</sup> [2 (GeV/c)<sup>2</sup>]. The dot-dashed curve at  $Q^2 = 0.40$  (GeV/c)<sup>2</sup> shows  $F_2$  obtained from the input valencelike quark distributions (i.e., valence and sea quarks) of Ref. [17]. Similarly, the dot-dashed curves at  $Q^2 = 1.40$  and  $3.00$  (GeV/c)<sup>2</sup> are evolved to  $Q^2$  values close to those of our  $F_2$  scaling curve. The dotted curve shows  $F_2$  obtained from the input valence-quark distributions from Ref. [17] only.

scaling curve at some  $\xi$  value will represent the average of proton resonance data for an extended ( $W^2, Q^2$ ) region, but that the average  $Q^2$  will globally increase with  $\xi$ . The curves shown represent the global fit to the world's deep inelastic data [16] for a fixed  $Q^2 = 10$  (GeV/c) $^2$  (NMC10, solid), and for a fixed  $Q^2 = 2$  (GeV/c) $^2$  (NMC2, dashed). Whereas the difference between the NMC fit for fixed  $Q^2 = 10$  (GeV/c) $^2$  and  $Q^2 = 2$  (GeV/c) $^2$  is small, and expected from logarithmic scaling violations, the difference between these NMC fits and our data [with  $Q^2 \approx 0.3$  (GeV/c) $^2$ ] derived from the duality-averaged scaling curve is dramatic at low  $\xi$ .

We have used the next-to-leading order calculations of Glück, Reya, and Vogt (GRV) [17] to investigate this in more detail. We use the GRV calculations since these are the only ones enabling us to evolve  $F_2$  down to the low momentum transfers of our measurements. In the GRV model, the shape of the gluon and quark-antiquark sea seen by experiment is dynamically generated through gluon bremsstrahlung. The GRV input distribution has been fixed by assuming only valence and valencelike (the input sea quark and gluon distributions also approach zero as  $x \rightarrow 0$ ) quark distributions at a finite  $Q^2$  value, constrained with appropriate  $Q^2$  evolutions to deep inelastic  $F_2$  data. We display in Fig. 2 the results of the calculations (GRV, dot-dashed), for  $Q^2$  values close to the average  $Q^2$  of our scaling curve. To compare with the very lowest  $\xi$  region of our data, we also show the *input* distribution itself at  $Q^2 = 0.40$  (GeV/c) $^2$ . Note that we here compare data and GRV calculations in a region not advocated by the authors, as "in the very low  $Q^2$  region below 1 (GeV/c) $^2$  nonperturbative higher-twist contributions are expected to become relevant" [18]. However, our assumption is that the higher-twist effects are reduced, if averaged over the full resonance region. The dotted curve in Fig. 2 denotes the GRV input distribution [at  $Q^2 = 0.40$  (GeV/c) $^2$ ] reflecting *only* the valence quark distributions (i.e., no sea quark contributions at all). One can verify that this input distribution is, at the lowest  $Q^2$  (i.e., lowest  $\xi$ ), even closer to the actual nucleon-resonance averaged data than the similar input distribution including valencelike effects (dot-dashed curve). The similarity of the various calculations, starting with the mentioned input distributions of Ref. [17], and the average scaling curve given by the nucleon resonance data, suggests that the duality-averaged scaling curve is dominated by valence-quark or valencelike quark contributions.

To verify this, we show in Fig. 3 a comparison of the averaged scaling curve from the deuterium resonance data (shaded band) with a selection of the world's data for the  $xF_3$  structure function. The  $xF_3$  structure function can be accessed by deep inelastic neutrino-iron scattering [19,20], and is associated with the parity-violating term in the hadronic current. Thus,  $xF_3$  measures in the quark-parton model the difference between quark and antiquark distributions, and is to first order insensitive to sea quark distributions. To enable a direct comparison, we have

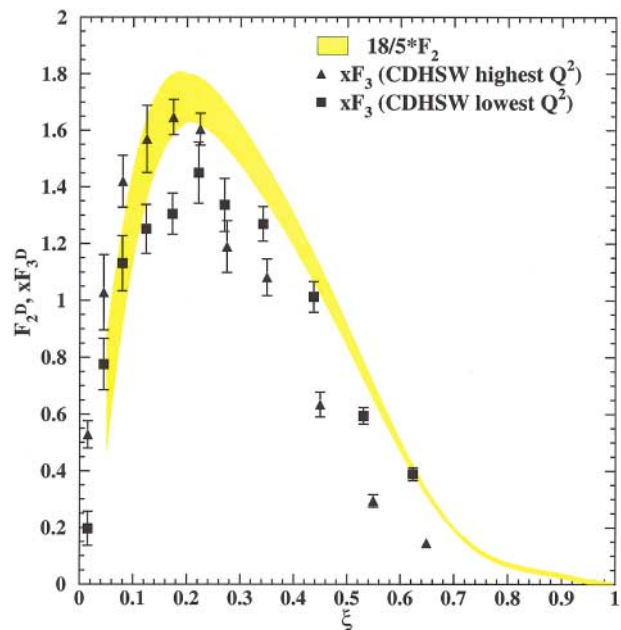


FIG. 3 (color). A comparison of the duality-averaged  $F_2$  scaling curve determined from the nucleon resonance region data from a deuterium target to the CDHSW data (Ref. [19]) on  $xF_3$  from deep inelastic neutrino-nucleus scattering data.

multiplied our average scaling curve by a factor of 18/5 to account for the quark charges, and have applied a straightforward nuclear correction to the  $xF_3$  data to obtain neutrino-deuterium data [21]. Although the agreement between the averaged  $F_2$  scaling curve of the deuterium resonance region and the deep inelastic neutrino  $xF_3$  data is not perfect, the similarity is striking. The observation of Bloom and Gilman that there may be a common origin between the electroproduction of resonances and deep inelastic scattering seems to be true for even the lowest values of  $Q^2$  if one assumes sensitivity to a valencelike quark distribution only. Since, at the lowest values of  $Q^2$ , one mainly excites the nucleon resonances, and hardly produces inelastic background (corresponding to the nonresonant meson production contributions), it is arguable that just the valencelike quarks are seen exciting the various nucleon resonances.

Alternatively, in a parton description, a possible interpretation for the strong  $Q^2$  dependence of  $F_2$  at low  $\xi$  and  $Q^2$  could be that, at very low  $Q^2$ , the large-wavelength probe is insensitive to coherent quark-antiquark pairs. This interpretation would be at odds with our usual parton description of the perturbative region of deep inelastic scattering, but could transcend the borderline between a parton description and nonperturbative QCD, which we investigate here. In deep inelastic scattering data, which for  $\xi \approx 0.1$  is typically at  $Q^2 > 1$  (GeV/c) $^2$ , the sea is indistinguishably intertwined with the  $F_2$  response. However, at our low  $Q^2$ , nonperturbative effects may readily appear in  $F_2$ , and are, in fact, required for  $Q^2 \rightarrow 0$ . The effect is further illustrated in Fig. 4. Here, the shaded bands indicate the

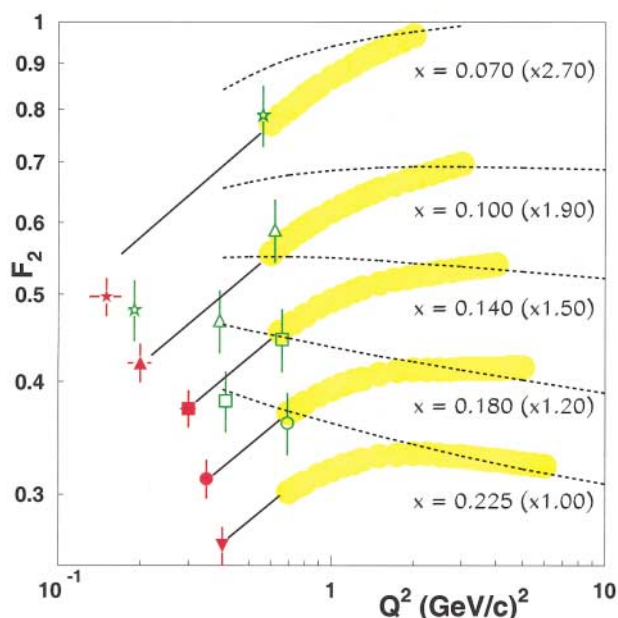


FIG. 4 (color). The low- $Q^2$   $F_2$  data for a region in  $x$  between 0.05 and 0.25. The shaded bands indicate the behavior of the deep inelastic data from Ref. [12]. The closed symbols represent data from the averaged  $F_2$  scaling curve of the proton resonance region. The open symbols represent data extracted from Ref. [14], with  $W^2 > 4 \text{ GeV}^2$ . Stars, triangles, squares, circles, and inverted triangles show data at  $x = 0.070, 0.100, 0.140, 0.180$ , and  $0.225$ , respectively. The solid curves are to guide the eye and represent a  $F_2 \sim 0.33 Q^{0.5}$  behavior. The dashed curves denote the  $Q^2$  evolution of  $F_2$  starting with the valencelike input distributions from Ref. [17].

range of data and uncertainty in existing high-precision deep inelastic measurements of  $F_2$  [12], at selected values of small  $x$ . The solid symbols represent the data extracted from this work, utilizing the averaged proton  $F_2$  scaling curve. The error bars here reflect the range in the  $x$  and  $Q^2$  value we use to obtain the scaling curve value at a certain  $\xi$ . The open symbols are values of  $F_2$  we extracted from Ref. [14]. These data are measured at invariant masses  $W^2 > 4 \text{ GeV}^2$ , and at low  $Q^2$  values [ $Q^2 < 1 (\text{GeV}/c)^2$ ]. We have assigned an uncertainty of 8% to these data, reflecting both the uncertainty in our extraction procedure and the normalization uncertainty of these older SLAC data. The data agree well with the shaded band of the more recent high-precision SLAC data. For these  $x$  values, the high- $W^2$ , low- $Q^2$ , SLAC data exhibit a  $Q^2$  dependence of the  $F_2$  structure function similar to that observed in our data. The combined data sample allows the conclusion that the observed effect is, to first order, independent of the  $W^2$  region.

The solid lines in Fig. 4 are just to guide the eye. We connected our datum at  $x = 0.14$  and  $Q^2 = 0.3 (\text{GeV}/c)^2$  with the SLAC data at similar  $x$  and  $Q^2 > 0.6 (\text{GeV}/c)^2$ . For other values of  $x$ , the lines have just been offset with the factor multiplying  $F_2$  for various  $x$ . The slopes of these lines happen to follow an  $F_2 = 0.33 Q^{0.5}$  behavior. Of course, it is likely that we just see an apparent  $F_2 \sim Q^{0.5}$  behavior in the limited  $Q^2$

region of our data, transcending the area between scaling at  $Q^2 > 1 (\text{GeV}/c)^2$  and the  $F_2 \sim Q^2$  expectation at  $Q^2 \rightarrow 0$ , based upon gauge invariance [6]. More data are needed to map the exact  $Q^2$  dependence at low  $Q^2$ , to investigate this point in detail. The dashed lines indicate the  $Q^2$  evolution of  $F_2$  starting from the valencelike input distributions of GRV [17,22]. It is clear that the calculations overshoot the low  $Q^2$  data, indicating the presence of a nonperturbative mechanism reducing the measured  $F_2$  structure function. This may be consistent with a turn-on of sensitivity to sea quarks.

In summary, we have measured inclusive electron-nucleon scattering cross sections in the resonance region for both hydrogen and deuterium targets, and have extracted the structure function  $F_2$  from these. The  $F_2$  data oscillate around an average scaling curve, down to the lowest  $Q^2$  measured. The average  $F_2$  scaling curve resembles deep inelastic  $x F_3$  structure function data. Our data suggest that the  $F_2$  structure function at these low momentum transfers follows the behavior of valencelike quarks only. In our kinematics, at intermediate  $x$  ( $\sim 0.1$ ) and low  $Q^2$  [ $\sim 0.3 (\text{GeV}/c)^2$ ], the structure function  $F_2$  still seems far from following an  $F_2 \sim Q^2$  behavior.

R. E. and C. E. K. thank J. Gomez, N. Isgur, and S. Liuti for helpful discussions. This work is supported in part by research grants from the U.S. Department of Energy and the U.S. National Science Foundation.

- [1] E. D. Bloom and F. J. Gilman, Phys. Rev. D **4**, 2901 (1971); Phys. Rev. Lett. **25**, 1140 (1970).
- [2] A. DeRujula, H. Georgi, and H. D. Politzer, Phys. Lett. **64B**, 428 (1976); Ann. Phys. (N.Y.) **103**, 315 (1977).
- [3] M. Virchaux and A. Milsztajn, Phys. Lett. B **274**, 221 (1992).
- [4] M. Glück, E. Reya, and A. Vogt, Z. Phys. C **53**, 127 (1992).
- [5] M. Glück, E. Reya, and A. Vogt, Phys. Lett. B **306**, 391 (1993).
- [6] A. Donnachie and P. V. Landshoff, Z. Phys. C **61**, 139 (1994).
- [7] I. Niculescu *et al.*, Phys. Rev. Lett. (to be published).
- [8] I. Niculescu, Ph.D. thesis, Hampton University, 1999.
- [9] D. Abbott *et al.*, Phys. Rev. Lett. **80**, 5072 (1998).
- [10] J. Arrington *et al.*, Phys. Rev. Lett. **82**, 2056 (1999).
- [11] F. E. Close, *An Introduction to Quarks and Partons* (Academic Press, Great Britain, 1979).
- [12] L. W. Whitlow *et al.*, Phys. Lett. B **250**, 193 (1990).
- [13] A. Bodek *et al.*, Phys. Rev. D **20**, 1471 (1979).
- [14] S. Stein *et al.*, Phys. Rev. D **12**, 1884 (1975).
- [15] O. Nachtmann, Nucl. Phys. **B63**, 237 (1975).
- [16] M. Arneodo *et al.*, Phys. Lett. B **364**, 107 (1995).
- [17] M. Glück, E. Reya, and A. Vogt, Eur. Phys. J. C **5**, 461 (1998).
- [18] E. Reya (private communication).
- [19] P. Berge *et al.*, Z. Phys. C **49**, 187 (1991).
- [20] E. Oltman *et al.*, Z. Phys. C **53**, 51 (1992); J. H. Kim *et al.*, Phys. Rev. Lett. **81**, 3595 (1998).
- [21] J. J. Aubert *et al.*, Nucl. Phys. **B293**, 740 (1987).
- [22] S. Liuti (private communication).